Макрогетероциклы
http://macroheterocycles.isuct.ru

DOI: 10.6060/mhc140714b

Electrocatalytic Reduction of Oxygen on Graphitized Carbon Electrode Modified with 5,15–Bis(pyrid–4–yl)–3,7,13,17–tetramethyl–2,8,12,18–tetraethylporphine and Its Cu^{II}, Fe^{III} Complexes

Do Ngoc Minh, Nadezhda M. Berezina,[@] Mikhail I. Bazanov, Aleksander S. Semeikin, and Aleksey V. Glazunov

Ivanovo State University of Chemistry and Technology, Research Institute of Macroheterocyclic Compounds, 153000 Ivanovo, Russia
[@]Corresponding author E-mail: sky_berezina@rambler.ru

The investigation of electrochemical properties of model electrodes with active layers containing 5,15-bis(pyrid-4-yl)-3,7,13,17-tetramethyl-2,8,12,18-tetraethylporphine (H_2(4-Py)$_2$TMeTEtP) and its Cu(II), Fe(III) complexes in 0.1 M KOH aqueous solution was carried out by cyclic voltammetry (CV). The potential ranges of oxidation-reduction processes related to the transformations of the porphyrin macrocycle, pyridyl moiety and central metal ion were established. The electrochemical parameters of oxygen electroreduction reaction (effective number of electrons - n, transfer coefficient - α, maximum potential - E_p, current density - j) were determined. It was shown that the electroreduction process of oxygen on electrode with dipyridylporphyrin and its Fe(III) complex occurs via 2-electron mechanism to give hydrogen peroxide ion, and for Cu(II) complex – via parallel-sequential pathway, including as 4-electron process with the rupture of the bond in molecular oxygen as 2-electron mechanism to give hydrogen peroxide ion (OH^- and HO_2^-).

Keywords: Pyridylporphyrins, metallocomplexes, electroreduction of molecular oxygen, cyclic voltammetry.

Электрокаталитическое восстановление кислорода на углеграфитовом электроде, модифицированном 5,15–бис(пирид–4–ил)–3,7,13,17–тетраметил–2,8,12,18–тетраэтилпорфином и его комплексами с Cu^{II} и Fe^{III}

Минь Нгок До, Н. М. Березина,[@] М. И. Базанов, А. С. Семейкин, А. В. Глазунов

Ивановский государственный химико-технологический университет, НИИ макрогетероциклических соединений, 153000 Иваново, Россия
[@]E-mail: sky_berezina@rambler.ru

Методом циклической вольтамперометрии (ЦВА) проведено исследование электрохимических свойств модельных электродов с активными слоями, содержащими 5,15-бис(пирид-4-ил)-3,7,13,17-тетраметил-2,8,12,18-тетраэтилпорфин и его комплексы с Cu(II) и Fe(III) в 0.1 М водном растворе КОН. Установлены области потенциалов протекания окислительно-восстановительных процессов, связанных с превращениями порфиринового макроцикла, пиридильного фрагмента и центрального иона металла. Определены электрохимические параметры для реакции электровосстановления молекулярного кислорода (эффективное число электронов - n, коэффициент переноса - α, потенциал максимума - E_p, плотность тока - j). Показано, что процесс электровосстановления кислорода на электроде с дипиридилпорфирином и Fe^{III}-комплексом протекает по двухэлектронному механизму с образованием пероксид-иона, а для Cu^{II}-комплекса – по параллельно-последовательному пути, включая как четырехэлектронный процесс с разрывом связи в молекуле кислорода, так и двухэлектронный механизм с образованием пероксид-иона (OH^- и HO_2^-).

Ключевые слова: Пиридилпорфирины, металлокомплексы, электровосстановление молекулярного кислорода, циклическая вольтамперометрия.

 © ISUCT Publishing

Introduction

The reduction reaction of molecular oxygen is one of the most important reactions in life processes (biological respiration) and in many electrochemical technologies such as chlor-alkaline electrolysis with air-depolarized cathodes,[1-3] metal-air batteries,[4] electrochemical sensors,[5,6] and *etc*.

Depending on the electrode material, its surface modification and the nature of the used catalysts, this reaction may take place both via 4-electron mechanism with the rupture of the O-O bond to give water (in acid medium) or hydroxide ion (in basic medium), and via 2-electron to generate hydrogen peroxide (in acid solutions) or hydrogen peroxide ion (in alkaline solutions). Normally, the oxygen reduction reaction (ORR) kinetics is slow. In order to speed up it, active catalysts are needed. Platinum-based materials are the most effective ones. However, because of their high cost, extensive research over the past several decades has focused on developing alternative catalytic systems. Such materials are non-noble metals,[7] carbon materials,[8,9] transition metal macroheterocyclic complexes, including porphyrins,[10,11] phtalocyanines and corroles,[12,13] metal oxides,[14] napthoquinone and anthraquinone derivatives[15-20] and others.

Pyridyl substituted porphyrins and their complexes with *d*-metals form a group of perspective catalysts in ORR due to the features of their chemical structure. Previously it was shown[21-23] that the introduction of pyridyl substituents into the porphyrin molecule has a positive effect on the electrocatalytic properties of these compounds in ORR in aqueous alkaline medium.

The electrochemical behavior of T(3-Py)P and T(4-Py)P[21,22] and mono(3-Py)TMeTEtP[23] in aqueous alkaline medium has been characterized in the course of electroreduction (electrooxidation) processes not only on the metal ion (Co, Cu , Fe) or the π-conjugated system of the macrocycle, but also on the electron-withdrawing (pyridyl) substituents, which are reduced in the potential range -0.7÷ -0.8 V (*vs*. Ag/AgCl electrode). The redox-behavior of electroactive pyridyl substituents are also discussed in [24].

The electrochemistry of TMePyP derivatives in non-aqueous media has been characterized largely with respect to the reduction which occurs not only at the metal and conjugated π-ring system of the macrocycle but also at 1-methyl-4-pyridyl substituents of the porphyrin ring which are electron deficient and electroreducible in the potential range of -0.2÷-1.0 V (*vs*. SCE). The most detailed electrochemical properties in non-aqueous media has been carried out for $[Mn^{III}(TMePyP)Cl]^{4+}$, $[Cu(TMePyP)]^{4+}$, $[Zn(TMePyP)]^{4+}$,[25] $[Co^{II}(TMePyP)]^{4+}$.[26,27] The reduction of the porphyrin macrocycle involves the simultaneous addition of two electrons. Also, due to the four positively charged substituents at the porphyrin periphery, the $[(TMePyP)]^{4+}$ (M = Mn, Co, Cu, Zn, and VO) are more difficult to be oxidized and easier to be reduced (400 ÷ 600 mV) then their phenyl analogs (M(TPhP)). The multi-electron transfer of electron upon reduction of methylpyridylporphyrins has been also reported in [27,28].

The electrochemistry of 16 different water-soluble porphyrins of $[M^{II}(TMePyP)]^{4+}(X^-)_4$ or $[M^{III}(TMePyP)Cl]^{4+}(Cl^-)_4$ type was reported in nonaqueous media where $X^- = Cl^-$ or BPh^{4-}. All the investigated compounds with electroinactive central metal ions undergo an overall addition of six electrons. This occurs for the most compounds via three two-electron-transfer steps, but more than three processes are observed for porphyrins having metal ions with a low electronegativity (*e.g.*, Cd(II)). Four of the compounds with electroactive central metal ions, $[M^{III}(TMePyP)Cl]^{4+}(Cl^-)_4$ (M = Co, Fe, Mn, or Au), undergo an additional reversible M(III)/M(II) process prior to reactions involving the porphyrin π-ring system and the 1-methyl-4-pyridyl substituents.[29]

The type and size of counter-ion should be irrelevant in water since porphyrins with TMePyP ring containing an M(II) or M(III) metal ion should exist in their dissociated form, *i.e.*, $[M^{II}(TMePyP)]^{4+}$ instead of $[M(TMePyP)]^{4+}(X^-)_4$ and $[M^{III}(TMPyP)X]^{4+}$ instead of $[M^{III}(TMePyP)X]^{4+}(X^-)_4$, under these solution conditions. In contrast, the type of counterion on the porphyrin moiety might affect the electrochemistry in nonaqueous solvents such as DMF, DMSO, or Py where the associated form may predominate in solution over the dissociated form due to the low polarity of the solvent.[29,30]

The electrochemical reduction of $H_2T(2\text{-Py})P$, $H_2T(3\text{-Py})P$ and $H_2T(4\text{-Py})P$ in acidic media has been reported in [31]. The 2- and 3-pyridyl derivative are reduced in two reversible one-electron steps, if one-electron product P(-I) H_4^+ of $H_2T(3\text{-Py})P$ unreacted. The $H_2T(4\text{-Py})P$ is reduced in a single two-electron step (-0.07 V *vs*. Ag/AgCl and gold electrode).[31]

In was shown[32-36] that metalloporphyrins and metallophthalocyanines activate a variety of electrochemical reactions. This is due to the nature of aromatic π-conjugated system of the macrocycle, conjugation of coordinated metal atom with this π-system and relatively ease to change the oxidation state of some of the central metal atom.

TPyP is found to be adsorbed irreversibly on Au(III) in acidic solution from -0.25 to 0.6 V (*vs*. SCE). The study of oxygen reduction reaction (ORR) in a homogeneous catalyst system of MT(Me-4-Py)P, M=Fe(III), Co(III), Mn(III) and Cu(II) in trifluoromethane sulfonic acid.[37] Except for Cu(II) T(Me-4-Py)P, no evidence of irreversible adsorption of metal complexes was found on the glassy carbon electrode. A model for outer-sphere catalysis involving superoxide ions ($2\ O^{-}$) as the initial species of the ORR followed by protonation reactions appears likely.

The study has shown[21,22] that the *meso*-pyridyl substitution of porphine (T(3-Py)P and T(4-Py)P) give a positive effect on its electrocatalytic activity in the reaction of molecular oxygen electroreduction, compared to their phenyl analogs in TPhP. Thus, the effect of depolarization of electroreduction process of molecular oxygen are 50 and 80 mV (*vs*. Ag/AgCl electrode) for electrodes $Co^{II}T(3\text{-Py})P$ and $Co^{II}T(4\text{-Py})P$ compared with $Co^{II}TPhP$ in aqueous alkaline medium. In opposite, the electrocatalytic activity of $Co^{II}(3\text{-Py})TMeTEtP$[23] is greater than that of $Co^{II}T(3\text{-Py})P$.[23] As one of the main reasons for the increase in catalytic activity, along with the electron-withdrawing effect of the pyridyl substituent, it was examined the impact of electronodonor alkyl substituents in the porphyrin. Among the studied T(3-Py)P, T(4-Py)P and (3-Py)TMeTEtP metal complexes most active ones in the reaction of oxygen electroreduction turned out to be those with Co(II) and Fe(III) while the lowest activity was shown by the Cu(II) complex, under these experimental conditions.

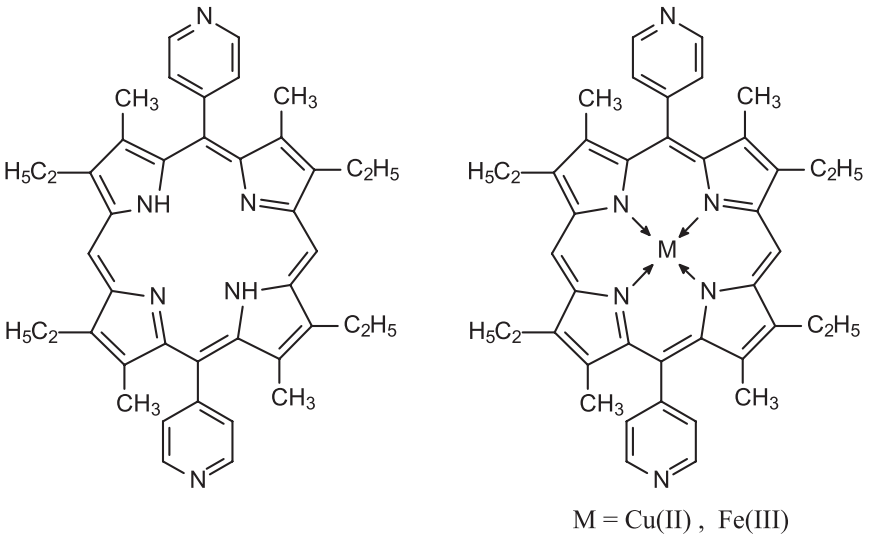

Figure 1. The structures of porphyrin ligand 5,15-bis(pyrid-4-yl)-3,7,13,17-tetramethyl-2,8,12,18-tetraethylporphine and its Cu^{II}, Fe^{III} complexes.

In the present work the results of studying electrochemical and electrocatalytic behavior of 5,15-bis(pyrid-4-yl)-3,7,13,17-tetramethyl-2,8,12,18-tetraethylporphine and its new Cu(II), Fe(III) complexes (Figure 1) were first reported. A nitrogen atom of the pyridyl group in molecules of studied catalysts, having a lone pair of electrons, favors the formation of bonds with electron-withdrawing molecules, cations, protons in acidic media, *etc*. Additionally, there are four methyl and four ethyl groups in the dipyridylporphyrin molecule having electron-donating effect with respect to the porphyrin macroring. The investigations have not been carried out of the dipyridylporphyrins redox properties.

Experimental

Porphyrin H_2(4-Py)$_2$TMeTEtP was synthesized according to the known method.[38]

Cu(II)-5,15-bis(pyrid-4-yl)-3,7,13,17-tetramethyl-2,8,12,18-tetraethylporphine, Cu^{II}(4-Py)$_2$TMeTEtP. The 10-fold excess of $Cu(CH_3COO)_2 \cdot H_2O$ was added to the solution of 50 mg (0.079 mmol) of ligand in 10 ml of DMF. The reaction mixture was refluxed for 2 hours under 153 °C, cooled. 15 ml of water and 1.5 ml of ammonia solution were added to the mixture. The residue was filtered, washed with water, and dried at 70 °C. Because of the formation of an outer sphere copper complex having polimeric nature, weight was given too high (0.069 g, 138 %) and the solubility in weakly polar solvents was reduced. To get the monomeric metallocomplex, polymer sample dissolved in 25 ml of chloroform and a solution of 0.2 g (0.56 mmol) of Trilon B in 3.0 ml of water was shaken, and then heated to 100 °C under stirring for 1 hour. The organic layer was separated, the solvent was evaporated, and the product was chromatographed on an aluminia column with chloroform as the elutant. Yield: 0.026 g (47 %). UV-vis ($CHCl_3$) λ_{max} nm (lgε): 408 (5.53); 533 (4.21); 569 (4.19). Data of the elemental analysis: found (calculated) for $CuC_{42}H_{42}N_6$, %: C – 71.85 (72.65); H – 5.98 (6.10); N – 11.96 (12.10).

(OAc)Fe(III)-5,15-bis(pyrid-4-yl)-3,7,13,17-tetramethyl-2,8,12,18-tetraethylporphine, Fe^{III}(4-Py)$_2$TMeTEtP. The 10-fold excess of iron powder was added to the solution of 50 mg (0.079 mmol) of ligand in 10 ml of CH_3COOH. The reaction mixture was refluxed for 2 hours, cooled. The iron powder was filtered. 20 ml of water was added to the complex solution, and then neutralized with an ammonia solution. The residue was filtered, dissolved in chloroform and chromatographed on an aluminia column with chloroform as the eluent. Yield: 0.030 g (55 %). UV-vis ($CHCl_3$) λ_{max} nm (lgε): 423 (5.23); 490 (3.78); 689 (3.56). Data of the elemental analysis: found (calculated) for (OAc)$FeC_{42}H_{42}N_6$, %: C – 70.50 (70.87); H – 5.98 (6.08); N – 11.00 (11.27).

The structure of the compounds was confirmed by electron spectroscopy and elemental analysis. UV-vis spectra were registered using SPEX SSP-715 spectrophotometer. The study of electrochemical behavior and catalytic properties in the electroreduction reaction of molecular oxygen for H_2(4-Py)$_2$TMeTEtP, Cu^{II}(4-Py)$_2$TMeTEtP and Fe^{III}(4-Py)$_2$TMeTEtP was performed by CV in 0.1 M KOH solution of the reagent grade. The measurements were carried out in a three-electrode electrochemical cell YASE-2 (Russian: ЯСЭ-2). Ag|AgCl,KCl(sat) and platinum electrodes were used as the reference and counter electrodes, respectively. The values of potentials were shown *vs.* this electrode in the text and graphics. The working electrode represented a graphitized carbon rod with the side surface insulated with a fluoroplastic coating. The working end of the rod (0.64 cm^2) was deposited with a layer (0.2–0.3 mm) of an active mass, which was prepared in an ethanol, involved the carbon support (TEC – technical elemental carbon P-514 (GOST 7885-86) with the ash content 0.45 %), the fluoroplastic suspension (6 % FP-4D) and the studied compound in the mass ratio of 7:2:1. The final heating of the active mass was performed at a temperature of 573 K within a minute. After ending experiments, the active mass was easily removed. The operation of new layer application could be repeated many times.

The measurements were performed using a potentiostat «PI 50-1» and a PC with a hardware-software complex. When studying redox reactions occurring on the surface of the original and porphyrins-modified electrodes, first of all the purging an electrolyte with argon (99.99 %) was conducted by bubbling (0.14 $ml \cdot s^{-1}$) for 40 minutes. Next, the working electrode was dipped in the electrolyte and cyclic *I,E*-curves were recorded in the potential range of 0.5÷-1.5 V. After completing the measurement under argon, the gaseous oxygen was bubbled through the solutions for 60 minutes. Potentials of cathodic (E_c) and anodic (E_a) peaks for observed processes with the participation of studied compounds were fixed with the accuracy of ±0.01 V. The values of redox

potentials were determined as the average in a series of 5–6 parallel experiments ($E_{red/ox} = \frac{E_c + E_a}{2}$).

Results and Discussion

Since the electroreduction reaction of molecular oxygen takes place at the interface «electrode – electrolyte solution» an important issue is to study the states of catalysts (porphyrin ligands and metalloporphyrins) in conditions, under which this reaction occurs.

Electrochemical Properties of Compound H_2(4-Py)$_2$TMeTEtP and its Cu, Fe Complexes

The Figure 2a shows the cyclic voltammograms of electrodes based on TEC (curve 1) and TEC with porphyrin H_2(4-Py)$_2$TMeTEtP (curve 2) in the active layer. *I,E*-curve for the electrode based on TEC has a high background current due to the large capacitive component of the porous electrode. When introducing porphyrins into the active mass, its specific surface[34] and the capacitive component decreases. After purging the electrolyte with argon on the cathodic part observed three peaks corresponding to the electroreduction processes of tetrapyrrole macrocycle (I_c, III_c) and pyridyl fragments (II_c) (Figure 2b). The reduction process of macrocycle III_c is irreversible. Because of proximity of the observed cathode processes I_c и II_c in potentials, this part of the voltammogram could be expanded to Gaussian components,[22] or subtraction of background current for electrodes before and after introducing porphyrins into the active mass could be build. In this case the second method is more reliable. Processing of experimental data by plotting the subtraction of background current (ΔI-E) for electrodes before and after introducing catalysts into the active mass (Figure 2b) allows to obtain curves with a sufficiently high resolution and amplitude of signals (from 100 to 300 μA) that is comparable or higher than the amplitude of signals obtained for experiments, where porphyrins are in soluble forms.[30]

As can be noted from Figure 2b, by increasing the cycling time (number of cycles), the amplitude of the current signal decreases somewhat. That could be due either to a partial exit of the studied compounds from the active mass in the bulk solution, or to the change in the hydrophilic-hydrophobic properties of the active layer. It should be noted that the observed changes in the current signal does not change the position of the potential peaks and these values of potentials for redox processes on porphyrins-modified electrodes are shown in Table 1. Assignment of the observed maxima to certain electrochemical processes was carried out on the basis of data given in the literature for compounds structurally related.[13,23,39-41] It was reported that in an alkaline medium for ligands without pyridyl substutients (H_2TMeTEtP and H_2TPhP) only two process of electroreduction were observed: the first peaks at E_{redox} = -0.74 V and -0.62 V, and the second – at -1.25 V and -1.03 V, respectively. For structurally related porphyrins containing pyridyl fragmemts (H_2(3-Py)HMeDEtP and H_2(4-Py)HMeDEtP) three electroreduction steps have been detected;[23,39] two of them are close to the E_{redox} values of H_2TMeTEtP and H_2TPhP, and are -0.73 V and -1.20 V. The third peak is observed at E_{redox} = -0.90 V for H_2(3-Py)HMeDEtP and E_{redox} = -0.95 V for H_2(4-Py)HMeDEtP in the CV-curves. It seems that, it may be associated with pyridyl substituents as these compounds don't have other structural differences.

For metal free porphyrin H_2(4-Py)$_2$TMeTEtP the first process I_c corresponds to the inclusion of the first electron to the macrocyclic π-electron system with formation of anion-radical, the second maximum is related to the reduction of pyridyl moieties to form dianionic form, and the third is associated with the localization of the third electron

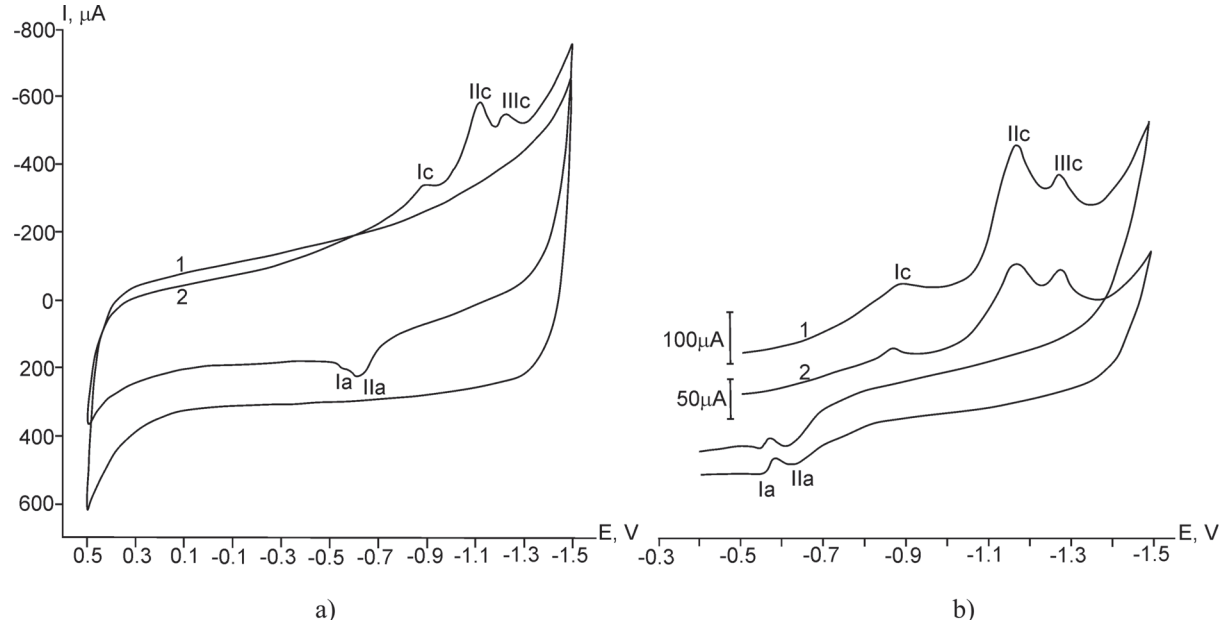

Figure 2. (a) *I,E*-curves for electrode, containing TEC (1) and TEC+H_2P (comp. H_2(4-Py)$_2$TMeTEtP) (2). The purge time of electrolyte of Ar – 40 min. The second cycle. Scan rate – 0.02 V·s^{-1}. (b) Different current characteristics (ΔI-E) for H_2P (comp. H_2(4-Py)$_2$TMeTEtP): 1 – second cycle, 2 – tenth cycle.

Table 1. Potentials of redox processes of electrodes with porphyrin compounds in 0.1 M KOH solution. Scan rate 0.02 V·s^{-1}.

Compound	$M^{n+}\leftrightarrow M^{(n-1)+}$			$L\leftrightarrow L^{-}$			$L^{-}\leftrightarrow L^{2-}$ Py			$L^{2-}\leftrightarrow L^{3-}$		
	$-E_c$	$-E_a$	$-E_{r/o}$	$-E^{I}_c$	$-E^{I}_a$	$-E^{I}_{r/o}$	$-E^{II}_c$	$-E^{II}_a$	$-E^{II}_{r/o}$	$-E^{III}_c$	$-E^{III}_a$	$-E^{III}_{r/o}$
H_2(4-Py)$_2$TMeTEtP	–	–	–	0.88	0.51	0.70	1.09	0.65	0.87	1.24	–	-
H_2TMeTEtP[41]	–	–	–	0.82	0.65	0.74	–	–	–	1.35	1.15	1.25
H_2TPhP[13]				0.66	0.56	0.62	–	–	–	1.08	0.97	1.03
H_2(3-Py)HMeDEtP[23]	–	–	–	0.86	0.60	0.73	1.07	0.73	0.90	1.23	1.16	1.20
H_2(4-Py)HMeDEtP[39]				0.87	0.60	0.74	1.21	0.70	0.95	1.33	–	–
Cu^{II}(4-Py)$_2$TMeTEtP	0.49	0.28	0.39	0.88	0.53	0.71	1.08	0.63	0.86	–	–	–
Fe^{III}(4-Py)$_2$TMeTEtP			$Fe^{3+}\rightarrow Fe^{2+}$ L→L^{-}				$L^{-}\leftrightarrow L^{2-}$ Py			$L^{2-}\leftrightarrow L^{3-}$		
	$-E_c$		$-E_a$		$-E_{r/o}$		$-E^{II}_c$	$-E^{II}_a$	$-E^{II}_{r/o}$	$-E^{III}_c$	$-E^{III}_a$	$-E^{III}_{r/o}$
	0.86		0.52		0.69		1.08	0.65	0.87	1.18	0.90	1.04

The values of potentials (V) are shown *vs*. Ag/AgCl electrode.

in the macrocycle to form a trianion. Electroreduction (electrooxidation) processes of dipyridylporphyrin may be presented by the scheme:

$$H_2P \cdot \underset{-e}{\overset{+e}{\rightleftharpoons}} \underset{\text{anion-radical form}}{H_2P^{\bullet}} \underset{-e}{\overset{+e}{\rightleftharpoons}} \underset{\text{dianion form}}{H_2P^{2-}} \xrightarrow{+e} \underset{\text{trianion form}}{H_2P^{3-}},$$

where P = porphyrin H_2(4-Py)$_2$TMeTEtP.

Similar Δ*I*-*E* dependences were constructed for copper and iron-containing complexes on the basis of experimental data (Figures 3, 4).

For the dipyridylporphyrin Cu(II) complex (Figure 3) the reduction process of the central metal is observed ($Cu^{2+} \leftrightarrow Cu^{+}$), and as well as two quasireversible processes of reduction of the macrocycle and pyridyl fragments (I_c, II_c). Electroreduction (electrooxidation) reactions of electrode containing copper porphyrin complex can be represented by the scheme:

$$Cu(II)P \underset{-e}{\overset{+e}{\rightleftharpoons}} [Cu(I)P] \underset{-e}{\overset{+e}{\rightleftharpoons}} \underset{\text{anion-radical form}}{[Cu(I)P]^{\bullet}} \underset{-e}{\overset{+e}{\rightleftharpoons}} \underset{\text{dianion form}}{[Cu(I)P]^{2-}},$$

where P = porphyrin H_2(4-Py)$_2$TMeTEtP.

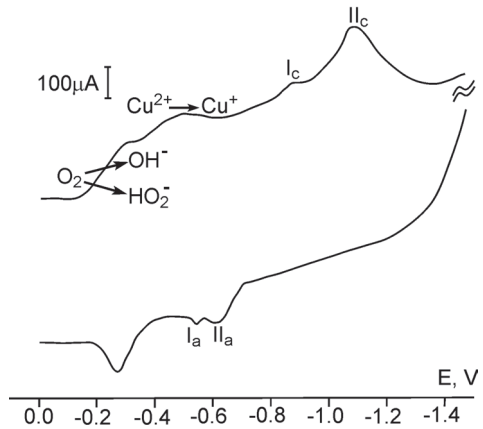

Figure 3. Δ*I vs*. *E* for Cu^{II}(4-Py)$_2$TMeTEtP. The second cycle. Scan rate – 0.02 V·s^{-1}. Ar.

For electrodes modified with (OAc)FeP when measuring the second cycle in the potential range (-0.4÷-0.9) V a sharp rise in the cathode current (Figure 4) is obseved, that is due to the superposition of the electrochemical reduction metal ion and tetrapyrrole macrocycle (I_c). Three peaks corresponding to the oxidation of the reduced forms of the complex are registered on the anodic part of voltammogram. The electrochemical tranformation of Fe-complex can be shown by scheme:

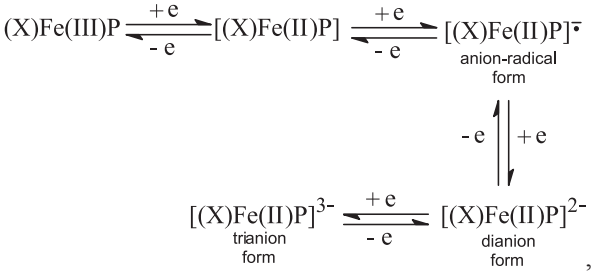

where X – extra-ligand, P = porphyrin H_2(4-Py)$_2$TMeTEtP.

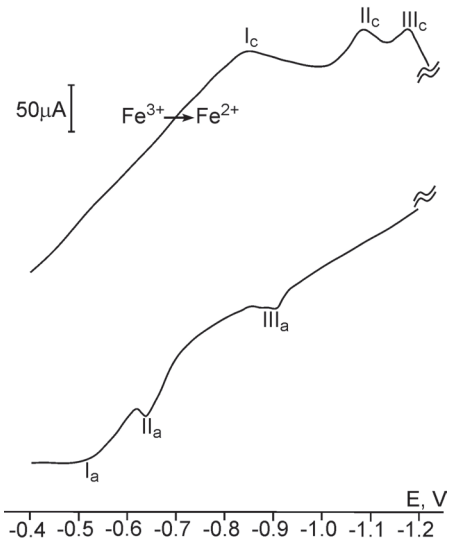

Figure 4. Δ*I vs*. *E* for Fe^{III}(4-Py)$_2$TMeTEtP. The second cycle. Scan rate – 0.02 V·s^{-1}. Ar.

The electrochemical parameters of the processes observed for electrodes modified with ligand H_2(4-Py)$_2$TMeTEtP and its Cu(II), Fe(III) complexes are presented in Table 1. According to the work[23] under the same experimental conditions for monopyridylporphyrin the electroreduction process of pyridyl moiety is characterized by redox-potential of -0.90 V, being close to the values for dipyridylporphyrin (Table 1). Therefore, it can be assumed that it is the pyridyl moiety in dipyridylporphyrin molecule that is reduced at this potential.

Electroreduction of Oxygen at the Surface of Electrode Modified with H_2(4-Py)$_2$TMeTEtP and Cu(II), Fe(III) Complexes

One of the objectives of the present work was the research of electroreduction reaction of molecular oxygen on electrodes modified with ligand H_2(4-Py)$_2$TMeTEtP and its Cu(II), Fe(III) complexes. To perform that, the cyclic voltammograms of the noted electrodes were registered under additionally purging the electrolyte with gaseous oxygen. The comparative analysis of voltammograms of studied compounds in the absence and in the presence of oxygen in solution showed, that when introducing oxygen to the solution the peaks on *I,E*-curves, which correspond to reduction (oxidation) processes of the porphyrin, remain. In addition, in the potential range of (-0.1÷-0.4) V on the cathodic part of *I,E*-curve a new current peak, that is associated with the electroreduction reaction of molecular oxygen (Figure 5), appears. The amount of current in the range of this maximum increases with purging time and reaches the maximum (constant) value at the time close to 60 minutes.

The dependences of current density of oxygen reduction on the electrodes potential containing carbon material and investigated compounds H_2(4-Py)$_2$TMeTEtP (Figure 6, curves 1-4) obtained by subtracting the currents in *I,E*-curves before the introduction of molecular oxygen into the electrolyte and after the continuous operation of the cathode of the curve. It is seen that the potentials of the maxima of

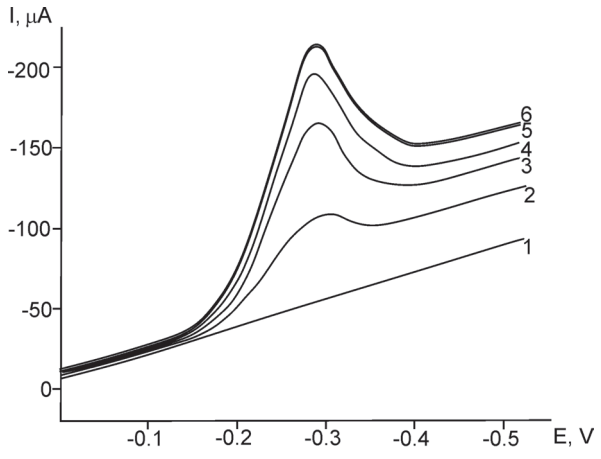

Figure 5. Fragments of a cathodic part of *I,E*-curves of the electrode with the compound H_2(4-Py)$_2$TMeTEtP upon the saturation of the solution with oxygen. Sweeping time, min: 1 – 0, 2 – 15, 3 – 30, 4 – 45, 5 – 60, 6 – 75.

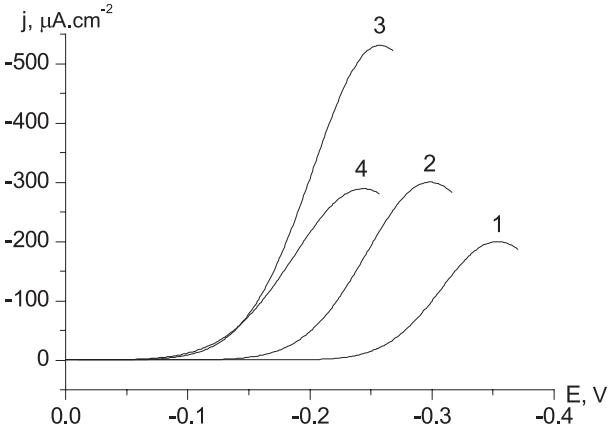

Figure 6. Dependence of the current density of reduction of molecular oxygen on the electrode potentials: 1 – without catalyst, 2 – H_2(4-Py)$_2$TMeTEtP, 3 – Cu^{II}(4-Py)$_2$TMeTEtP, 4 – Fe^{III}(4-Py)$_2$TMeTEtP. Purge time – 60 min. Scan rate – 0.02 V·s^{-1}.

these processes for TEC and compound H_2(4-Py)$_2$TMeTEtP are -0.35 V and -0.30 V, respectively. Moreover, the electrode based on carbon material provides a peak current being slightly lower comparing with electrode with porphyrin ligand. Decrease in overpotential of 50 mV, as well as shift in halfwave potential $E_{1/2}(O_2)$ of 60 mV and an enhancement of current density on electrode in the present of ligand H_2(4-Py)$_2$TMeTEtP indicate an electrocatalytic process.

It was established that by increasing the sweep rate of potentials, the peak current for reduction of O_2 (I_p) increases and is proportional to the square root of the scan rate ($\sqrt{\upsilon}$) (Figure 7a, curve 1) according to the equation:

$$I_p = 1.38\upsilon^{1/2},\ R^2 = 0.998. \qquad (1)$$

When building the experimental data in the coordinates $\lg I_p$–$\lg\upsilon$ (Figure 7b, curve 1), the linear dependence corresponding to the following equation is observed.

$$\lg I_p = 0.14 + 0.50(\lg\upsilon),\ R^2 = 0.998. \qquad (2)$$

The slope of the equation (2) amounts to 0.5, which corresponds to the theoretically expected value for processes, in which reacting species diffuse toward the electrode without being specifically adsorbed.[42] It's stressed that the peak potential of the catalytic reduction of oxygen (E_p) is shifted into the cathode region by increasing the sweep rate (Figure 7c, curve 1). Furthermore, the plot $E_p = f(\lg\upsilon)$ is linearized by the equation:

$$E_p = -0.43 - 0.07(\lg\upsilon),\ R^2 = 0.984. \qquad (3)$$

These linear dependences that are characteristic for the irreversible processes confirm that the oxygen reduction reaction under experimental conditions is irreversible process.

In order to obtain the information about the rate-limiting step of charge transfer, the Tafel slope is calculated according to the equation (4) binding the peak potential (E_p) and the scan rate (υ), characterizing the irreversible electrode process.[43]

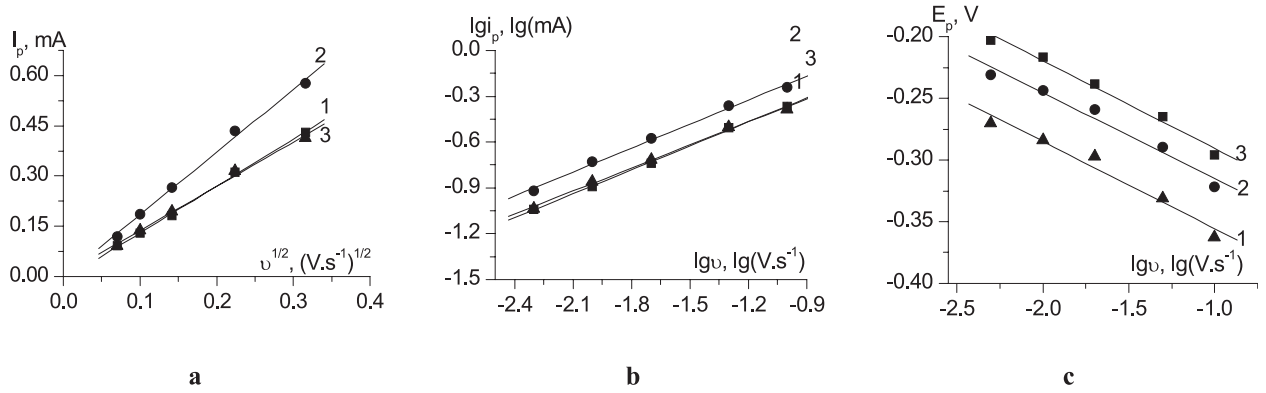

Figure 7. (a) Plots of I_p *vs*. $\upsilon^{1/2}$. (b) Plots of $\lg I_p$ *vs*. lgυ. (c) Plots of E_p *vs*. lgυ of electrodes with H_2(4-Py)$_2$TMeTEtP (1), Cu^{II}(4-Py)$_2$TMeTEtP (2), Fe^{III}(4-Py)$_2$TMeTEtP (3).

$$E_p = E^{o'} - \frac{RT}{\alpha n_c}\left[0.780 + \ln\left(\frac{D_0^{1/2}}{k}\right) + \ln\left(\frac{\alpha n_c F \upsilon}{RT}\right)^{1/2}\right] \qquad (4),$$

where $E^{0'}$ – the formal potential (V); α – the transfer coefficient; n_c – the number of electrons exchanged in the rate-determining step; D_0 – the diffusion coefficient of the oxidant ($cm^2 \cdot s^{-1}$); k – the heterogeneous rate constant of electron transfer ($cm \cdot s^{-1}$); υ – the scan rate ($V \cdot s^{-1}$).

The equation (4) may be peformed in a simplified way:

$$E_p = const - \frac{b}{2}\lg \upsilon \qquad (5),$$

where $b = \frac{2.303RT}{\alpha n_c F}$ – Tafel slope.

The slope of plot $E_p = f(\lg\upsilon)$ (Figure 7c) amounts to –0.5*b*. The value $b = -2\partial E/\partial(\lg\upsilon)$ makes up 0.140 V (140 mV), and $\alpha n_c = 0.42$. Consequently, the rate-limiting step is a one-electron transfer, assuming that the transfer coefficient (α) is equal to 0.42. It must be stressed that it is the first electron that is attached to oxygen molecule in this step.

In order to determine the pathway of the occurrence of oxygen reduction reaction on the electrode modified with porphyrin H_2(4-Py)$_2$TMeTEtP, the overall numbers of the transferred electrons per oxygen molecule (*n*) was calculated. For this, the equation (6) for irreversible processes[44] was applied.

$$i_p = 2.99 * 10^5 n\sqrt{\alpha n_c} S C_o \sqrt{D_o \upsilon} \qquad (6),$$

where *n* – the total number of electrons participating in the oxygen reduction reaction; *S* – the surface area of the electrode (cm^2); C_0 – the bulk concentration of oxygen ($mol \cdot l^{-1}$); D_0 – the diffusion coefficient of oxygen ($cm^2 \cdot s^{-1}$); υ – the scan rate ($V \cdot s^{-1}$).

The following values of parameters in the equation (6) are used in the calculation: S = 0.64 cm^2; $C_0 = 1.2 \cdot 10^{-3}$ $mol \cdot l^{-1}$;[44] $D_0 = 1.9 \cdot 10^{-5}$ $cm^2 \cdot s^{-1}$.[45] The obtained values of *n* at different scan rates are shown in Table 2. Calculations show that the electroreduction reaction of O_2 on the electrode containing the compound H_2(4-Py)$_2$TMeTEtP takes place via 2-electron pathway to give hydrogen peroxide anion.

A similar analysis of the experimental data was performed for metallocomplexes Cu^{II}(4-Py)$_2$TMeTEtP and Fe^{III}(4-Py)$_2$TMeTEtP (Figure 7, Tables 2, 3). The results show that the electroreduction reaction of oxygen on the electrode modified with complex Fe^{III}(4-Py)$_2$TMeTEtP occurs via 2-electron

Table 2. Peak currents of oxygen reduction and the number of electrons transferred in the given process at different scan ran.

Scan rate υ, $mV \cdot s^{-1}$	H_2(4-Py)$_2$TMeTEtP		Cu^{II}(4-Py)$_2$TMeTEtP		Fe^{III}(4-Py)$_2$TMeTEtP	
	I_p, mA	n	I_p, mA	n	I_p, mA	n
5	0.090	2.0	0.120	2.6	0.092	2.0
10	0.140	2.1	0.190	2.9	0.130	2.0
20	0.190	2.1	0.260	2.9	0.190	2.0
50	0.320	2.1	0.440	3.0	0.310	2.2
100	0.410	2.0	0.580	2.8	0.430	2.1

Table 3. Plots of I_p *vs* $\upsilon^{1/2}$, $\lg I_p$ *vs* lgυ, E_p *vs* lgυ.

Compound	H_2(4-Py)$_2$TMeTEtP	Cu^{II}(4-Py)$_2$TMeTEtP	Fe^{III}(4-Py)$_2$TMeTEtP
I_p *vs* $\upsilon^{1/2}$	$I_p = 1.38\upsilon^{1/2}$, $R^2 = 0.998$	$I_p = 1.87\upsilon^{1/2}$, $R^2 = 0.998$	$I_p = 1.40\upsilon^{1/2}$, $R^2 = 0.999$
$\lg I_p$ *vs* lgυ	$\lg I_p = 0.14+0.50$ (lgυ), $R^2 = 0.998$	$\lg I_p = 0.27+0.50$(lgυ), $R^2 = 0.997$	$\lg I_p = 0.15+0.50$ (lgυ), $R^2 = 0.999$
E_p *vs* lgυ	$E_p = -0.43 - 0.07$(lgυ), $R^2 = 0.984$	$E_p = -0.38 - 0.07$ (lgυ), $R^2 = 0.985$	$E_p = -0.36 - 0.07$(lgυ), $R^2 = 0.993$

Table 4. Kinetics parameters of oxygen reduction process.

Compound	$-E(O_2)$, V*	j, mA·cm^{-2}**	n	α
TEC	0.32	0.004	2.0	–
H_2(4-Py)$_2$TMeTEtP	0.24	0.050	2.1	0.41
Cu^{II}(4-Py)$_2$TMeTEtP	0.17	0.319	2.9	0.43
Fe^{III}(4-Py)$_2$TMeTEtP	0.18	0.217	2.0	0.42

*Values of potential for oxygen reduction at j = 0.15 mA·cm^{-2} and υ = 0.02 V·s^{-1}
**Values of current density at an electrode potential -0.2 V and υ = 0.02 V·s^{-1}

pathway ($n \approx 2$); and with complex Cu^{II}(4-Py)$_2$TMeTEtP – via parallel pathways to yield HO_2^- and OH^- ($n \approx 3$).

In order to assess the electrocatalytic activity of the studied porphyrins in the reduction reaction of O_2 a current density (j) at the constant value of electrode potential (-0.2 V), and the amounts of potentials for reduction wave of O_2 at fixed current density $E(O_2)$ (Table 4) were defined. It is seen that during the transition from the porphyrin ligand to the metallocomplexes the value of j increases, and $E_{1/2}(O_2)$ is shifted to the range of positive potentials. A rise of the electrochemical effect of studied catalysts is observed in the row: H_2(4-Py)$_2$TMeTEtP < Fe^{III}(4-Py)$_2$TMeTEtP < Cu^{II}(4-Py)$_2$TMeTEtP (Figure 6). The insufficiently high activity of the Fe-complex may be due to the participation of the oxidized form (Fe(III)) and the present of an extra-ligand (CH_3COO^-) promoting the shielding of the active center of adsortion and electroreduction for molecular oxygen.

Conclusions

The potential ranges of redox processes related to conversion of the porphyrin macrocycle, the pyridyl moiety and the central metal ion were established. It was shown that the electroreduction reaction of oxygen on the electrodes with 5,15-bis(pyrid-4-yl)-3,7,13,17-tetramethyl-2,8,12,18-tetraethylporphine and its Cu(II), Fe(III) complexes in 0.1 M KOH solution is irreversible. The rate-limiting step is the first electron transfer from the electrode to molecule O_2. Dipyridylporphyrin and its Fe(III) complex promote speeding up the electroreduction process of O_2 via 2-electron mechanism, and Cu(II) complex directs the course of process simultaneously via 2- and 4-electron mechanism.

Acknowledgments. The work was financially supported by Russian Science Foundation, the agreement № 14-23-00204 and Ministry of Education and Science of Russia in the framework of the state task.

References

1. Steele B.C.H., Heinzel A. *Nature* **2001**, 414, 345-352.
2. Spendelow J.S., Wieckowski A. *Phys. Chem. Chem. Phys.* **2007**, *9*, 2654-2675.
3. Lipp L., Gottesfeld S., Chlistunoff J. *J. Appl. Electrochem.* **2005**, *35*, 1015-1024.
4. Lee J., Kim S.T., Cao R., Choi N., Liu M., Lee K.T., Cho J. *Adv. Energ. Mater.* **2011**, *1*, 34-50.
5. Ramamoorthy R., Dutta P.K., Akbar S.A. *J. Mater. Sci*. **2003**, *38*, 4271-4282.
6. Correia M.J., Pereira E.V., Salta M.M., Fonseca I.T.E. *Cem. Concr. Compos.* **2006**, *28*, 226-232.
7. Zhang L., Zhang J., Wilkinson D.P., Wang H. *J. Power Sources* **2006**, *156*, 171-182.
8. Brito P.S.D., Sequeira C.A.C. *J. Power Sources* **1994**, *52*, 1-16.
9. Xu J., Huang W.H., McCreery R.L. *J. Electroanal. Chem.* **1996**, *410*, 235-242.
10. Zhutaeva G.V., Tarasevich M.R., Radina M.V., Chenyshova I.S. *Russ. J. Electrochem.* **2009**, *45*, 1080-1088.
11. Collman J.P., Kim K. *J. Am. Chem. Soc.* **1986**, *108*, 7847-7849.
12. Zagal J.H., Griveau S., Francisco Silva J., Nyokong T., Bedioui F. *Coord. Chem. Rev.* **2010**, *254*, 2755-2791.
13. Bazanov M.I., Berezina N.M., Karimov D.R., Berezin D.B. *Russ. J. Electrochem.* **2012**, *48*, 905-910.
14. Jorissen L. *J. Power Sources* **2006**, *155*, 23-32.
15. Chan Pham M., Dubois J.-E. *J. Electroanal. Chem.* **1986**, *199*, 153-164.
16. Degrand C. *J. Electroanal. Chem.* **1984**, *169*, 259-268.
17. Katz E., Schmidt H.-L. *J. Electroanal. Chem.* **1994**, *368*, 87-94.
18. Golabi S.M., Raoof J.B. *J. Electroanal. Chem.* **1996**, *416*, 75-82.
19. Li Y., Lenigk R., Wu X., Gruendig B., Dong S., Renneberg R. *Electroanalysis* **1998**, *10*, 671-676.
20. Salimi A., Eshghi H., Sharghi H., Golabi S.M., Shamsipur M. *Electroanalysis* **1999**, *11*, 114-119.
21. Berezina N.M., Bazanov M.I., Semeikin A.S. *Izv. Vyssh. Uchebn. Zaved., Khim. Khim. Tekhnol.* **2010**, *53*(1), 32-36 (in Russ.).
22. Berezina N.M., Bazanov M.I., Semeikin A.S., Glazunov A.V. *Russ. J. Electrochem.* **2011**, *47*(1), 46-51.
23. Berezina N.M., Bazanov M.I., Do Ngoc Minh, Semeikin A.S. *Izv. Vyssh. Uchebn. Zaved., Khim. Khim. Tekhnol.* **2012**, *55*, 45-50 (in Russ.).
24. Brisach-Wittmeyer A., Lobstein S., Gross M., Giraudeau A. *J. Electroanal. Chem*. **2005**, *576*, 129-137.
25. Van Caemalbecke E., Kutner W., Kadish K.M. *Inorg. Chem*. **1993**, *32*, 438-444.
26. Sazou D., Araullo-McAdams C., Han B.C., Franzen M.M., Kadish K.M. *J. Am. Chem. Soc*. **1990**, *112*, 7879-7886.
27. Araullo-McAdams C., Kadish K.M. *Inorg. Chem.* **1990**, *29*, 2749-2757.
28. Chen F.-C., Cheng S.-H., Yu C.-H., Liu M.-H., Su Y.O. *J. Electroanal. Chem.* **1999**, *474*, 52-59.
29. Kadish K.M., Royal G., Van Caemelbecke E., Gueletti L. Metalloporphyrins in Non-Aqueous Media: Database of Redox Potentials. *In: The Porphyrin Handbook* (Kadish K.M., Smith K.M., Guilard R., Eds.) New York: Acad. Press, **2000**, Vol. 9, pp. 1-219.
30. Van Caemelbecke E., Derbin A., Hambright P., Garsia R., Doukkali A., Saoiabi A., Ohkudo R., Fukuzumi S., Kadish K.M. *Inorg. Chem*. **2005**, *44*, 3789-3798.
31. Neri B.P., Wilson G.S. *Anal. Chem.* **1973**, *45*, 442-445.
32. Ye T., He Y., Borguet E. *J. Phys. Chem. B* **2006**, *110*, 6141-6147.
33. Tarasevich M.R., Radyushkina K.A. *Catalysis and Electrocatalysis by Metalloporphyrins*. Moscow: Nauka, **1982**. 168 p. (in Russ.) [Тарасевич М.Р., Радюшкина К.А. *Катализ и электрокатализ металлопорфиринами*. М: Наука, **1982**. 168 с.].
34. Tarasevich M.R., Radyushkina K.A., Bogdanovskaya V.A. *Electrochemistry of Porphyrins*. Moscow: Nauka, **1991**.

312 p. (in Russ.) [Тарасевич М.Р., Радюшкина К.А., Богдановская В.А. *Электрохимия порфиринов*. М.: Наука, **1991**. 312 с.]
35. Ji Yanfeng, Li Zhongfang, Wang Suwen, Xu Guofeng, Li Degang, Yu Xianjin *J. Electrochem. Soc*. **2011**, *158*, B139-B1242.
36. Masa J., Ozoemena K., Schuhmann W., Zagal J.H. *J. Porphyrins Phthalocyanines* **2012**, *16*, 761-784.
37. He Q., Mugadza T., Hwang G., Nyokong T. *Int. J. Electrochem. Sci.* **2012**, *7*, 7045-7064.
38. Ivanova Yu.B., Semeikin A.S., Glazunov A.V., Mamardashvili N.Zh. *Russ. J. Org. Chem.* **2010**, *46*, 917-923.
39. Minh Do Ngoc, Berezina N.M., Bazanov M.I., Semeikin A.S., Glazunov A.V. *Macroheterocycles* **2014**, *7*, 73-79.
40. Bazanov M.I., Petrov A.V. *Organic Metal Complexes: Electrochemistry, Electrocatalysis, Thermochemistry*. Ivanovo: IIGPS MCHS Rossii, **2007**. 174 p. (in Russ.) [Базанов М.И., Петров А.В. Органические комплексы с металлами: электрохимия, электрокатализ, термохимия. Иваново: ИИГПС МЧС России, **2007**. 174 с.].
41. Bazanov M.I., Petrov A.V. In: *Advances in Porphyrin Chemistry*, Vol. 5. (Golubchikov O.A., Ed.), SPb.: NII, St. Petersburg State University, **2007**. pp. 275-292 (in Russ.) [Базанов М.И., Петров А.В. В кн.: *Успехи химии порфиринов*, Т. 5 (Голубчиков О.А., ред.), Спб.: Изд-во НИИ химии СПБГУ, **2007**. с. 275-292].
42. Gosser D.K., Jr. *Cyclic Voltammetry: Simulation and Analysis of Reaction Mechanisms*. New York: VCH, **1993**. 154 p.
43. Bard A.J., Faulkner L.R. *Electrochemical Methods: Fundamentals and Applications (2nd Edn.)*. New York: Wiley, **2000**. 833 p.
44. Scholz F., *et al. Electroanalytical Methods: Guide to Experiments and Applications*. Berlin, Heidelberg, New York: Springer, **2010**. 359 p.
45. Davis R.E., Horvath G.L., Tobias C.W. *Electrochimica Acta* **1967**, *12*, 287-297.

Received 05.07.2014
Accepted 20.03.2015